Microstructure and viscoelasticity of confined semiflexible polymer networks

M. M. A. E. CLAESSENS[1], R. THARMANN[1], K. KROY[2,3] AND A. R. BAUSCH[1]*

[1]E22-Biophysics, Technische Universität München, James Franck Straße, 85748 Garching, Germany
[2]Institut für Theoretische Physik, Universität Leipzig, Postfach 100920, 04009 Leipzig, Germany
[3]Hahn-Meitner Institut, Glienicker Straße 100, 14109 Berlin, Germany
*e-mail: abausch@ph.tum.de

Published online: 26 February 2006; doi:10.1038/nphys241

The rapidly decreasing dimensions of many technological devices have spurred interest in confinement effects[1]. Long before, living organisms invented ingenious ways to cope with the requirement of space-saving designs down to the cellular level. Typical length scales in cells range from nanometres to micrometres so that the polymeric constituents of the cytoskeleton are often geometrically confined. Hence, the mechanical response of polymers to external confinement has potential implications both for technology and for our understanding of biological systems alike. Here we report a study of *in vitro* polymerized filamentous actin confined to emulsion droplets. We correlate observations of the microstructure, local rheological properties and single-filament fluctuations. Enforcing progressively narrower confinement is found to induce a reduction of polymer fluctuations, network stiffening, structural heterogeneities and eventually cortex formation. We argue that the structural and mechanical effects can be consistently explained by a gradual suppression of single-polymer eigenmodes.

Generally speaking, confinement effects can be expected whenever an externally constrained dimension matches a characteristic internal length scale of the confined system such as the end-to-end distance R or the radius of gyration or the persistence length l_p of a single polymer, or the size of the correlation or entanglement unit in a semidilute polymer solution. What sort of mechanical response one should theoretically expect in either case is not *a priori* obvious and might well depend sensitively on the confinement geometry. At the same time, it presents formidable experimental challenges to separately resolve the various scales in measurements and, therefore, despite considerable theoretical progress[2], experimental studies with synthetic polymers could not yet establish a complete picture of confinement effects on the nanoscale[3,4]. Biopolymer networks, on the other hand, are accessible to optical techniques and microrheometry. A versatile model system is provided by F-actin, a semiflexible biopolymer with typical contour lengths up to tens of micrometres and a persistence length of $l_p \approx 17$ μm. *In vivo*, F-actin forms a geometrically confined two-to-three-dimensional network, the cytoskeleton, which stabilizes the cell and is largely responsible for its viscoelastic behaviour. *In vitro* polymerized entangled and crosslinked actin networks have therefore been used extensively as model systems to attain a better understanding of the mechanical properties of cells (see, for example, refs 5,6 and references therein). In bulk solutions and gels, the viscoelastic mechanical response of actin is determined by the thermally excited bending undulations of the filaments. Similar to rubber, the elastic response of the network is predominantly entropic and is expected to be very sensitive to anything that hinders the thermal fluctuations of the polymers. Indeed, the spatial organization of actin networks in giant vesicles was reported to depend on the membrane composition, the vesicle radius and the filament length[7–9]. In small vesicles, filaments were observed to predominantly form a fuzzy cortex concentrated near the membrane, whereas a homogeneous actin network was found in larger vesicles[9]. However, it is difficult to control such vesicles and, therefore, the consequences of purely geometrical confinement on the mechanical properties of actin networks have not yet been addressed systematically.

Here, we introduce an alternative method for encapsulating actin networks by phospholipid-stabilized emulsion droplets in which the filaments move freely at the wall, which is clearly demonstrating that the walls do not act as pinning sites, but rather as steric constraints (see the Supplementary Information). We observed homogeneous bulk networks in large drops and a fuzzy cortex forming underneath the drop surface in small drops. In good agreement with earlier studies with vesicles, where the membranes contained cholesterol to avoid physisorption of actin at the walls[9], we found that cortex formation only starts below a well-defined droplet diameter $D_c \approx 12$–13 μm. To quantify the heterogeneity of the networks, we measured the pore size distribution by a diffusing bead technique (see the Methods section). For example, for solutions of actin concentration $c_a = 1.2$ mg ml^{-1} the mean mesh size was estimated as $\xi \approx 0.23$ μm with a half width σ of 0.07 μm for droplets with $D \approx 16$ μm and $\xi \approx 0.23$ μm, $\sigma \approx 0.04$ μm for $D \approx 148$ μm. Altogether, we found that for droplets

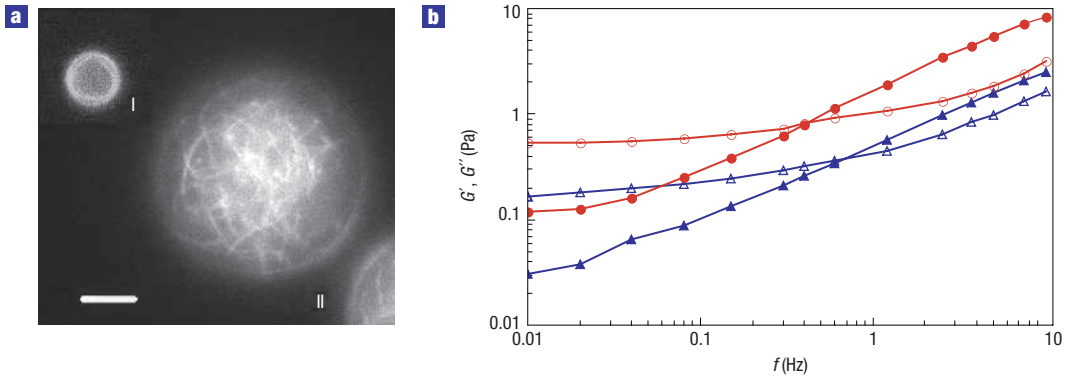

Figure 1 Actin solutions encapsulated in sufficiently small emulsion droplets are locally more heterogeneous and more elastic than bulk solutions. a, Fluorescent micrographs of emulsion droplets containing rhodamine phalloidin-labelled actin filaments. In small droplets ($D \leq 12$ μm), the actin is organized in a cortex close to the droplet surface (I), whereas it is more homogeneously distributed in large droplets (II). The scale bar is 10 μm. **b**, The effective (locally measured) storage modulus $G'(\omega)$ (open symbols) and the loss modulus $G''(\omega)$ (filled symbols) of confined actin networks in emulsion droplets of diameters $D = 20$ μm (open circles and filled circles) and $D = 133$ μm (open triangles and filled triangles), respectively. Data are shown for an actin concentration of 1.2 mg ml^{-1} and a ratio of actin to gelsolin $r_{A:G}$ of 7,770:1.

of diameters less than $D \approx 30$ μm but larger than D_c the network became more heterogeneous.

To test whether these heterogeneities also increased the networks stiffness we used active microrheology to determine the local moduli. For ease of comparison with macrorheometric data, it is customary to represent the locally measured susceptibilities in the form of frequency-dependent local storage and loss moduli, G', G''. Typical examples for the frequency-dependent 'local moduli' thus obtained by the active technique for the confined actin networks are shown in Fig. 1b. In the large droplet ($D = 133$ μm), where no confinement effects are expected (contour length $L \approx 21$ μm, $l_p \approx 17$ μm), the local moduli are similar to those observed for bulk actin solutions[10] in both magnitude and dependence on actin concentration. In smaller droplets ($D = 20$ μm), both G' and G'' are observed to increase significantly. The frequency dependence of the moduli, however, remains essentially unchanged: the frequency where G' and G'' intersect, the slope of the plateau in G' and the scaling of G'' at the highest measured frequencies are found to be comparable for all droplet diameters. We tested with passive microrheology using latex beads in the diameter range of 500 nm to 4 μm that the onset of the network hardening was independent of the bead size (data not shown). Even in small droplets, the network organization was not observably affected by the presence of probe particles. The main effect of confinement on the microrheological properties, therefore, seems to be a shift in the overall energy scale, given by the plateau elastic modulus G^0. This intriguing observation of an essentially invariant functional form of the moduli under confinement could possibly indicate that our highest frequencies are still far below the so-called high-frequency regime, which is predicted to arise from independent single-polymer contributions[11,12]. Alternatively, it may be interpreted as evidence that the effects of confinement on the single-polymer response (at high frequencies) and on the local collective rheological properties (at low frequencies) are intimately linked. Figure 2a shows $G^0 \equiv G'$ (0.01 Hz) as a function of the droplet diameter D for actin concentrations of 0.6 and 1.2 mg ml^{-1}. For both concentrations, G^0 was found to be independent of the droplet diameter for $D > 30$ μm, whereas on further confinement G^0 was observed to increase significantly. In contrast, for solutions consisting of filaments with a mean length of 5 μm, G^0 was found to be independent of D down to the smallest droplet diameters that could be tested (not shown). This strongly suggests that the confinement effects set in when the characteristic confining linear dimension approaches the end-to-end distance R, which seems to be in accord with observations of a similar increase in the viscoelastic moduli for flexible polymers[3,4], although the interpretation remained somewhat inconclusive in the latter case.

We propose to apply concepts originally developed for the bulk plateau shear modulus of semiflexible polymer solutions to rationalize the increase in elasticity with increasing geometrical confinement of the actin solutions (see ref. 13 for an overview). The microscopic origin of the rubber plateau is the strong confinement of entangled polymers to tube-like regions on intermediate timescales; from seconds up to many minutes for F-actin. In contrast to crosslinked networks, where the affine stretching of single filaments can well account for the observed viscoelastic properties[14,15], the response of entangled solutions without crosslinks is thought to be dominated by a lateral confinement of the thermal bending undulations[10,16,17]. The corresponding prediction for the bulk plateau modulus is $G^0 \approx k_B T / V_e$, where k_B is Boltzmann's constant, T is temperature and V_e is the average volume per binary filament collision that decreases with monomer concentration c_a as $V_e \sim c_a^{-7/5}$ in bulk solutions, which explains very well the macroscopically measured scaling $G^0 \sim c_a^{7/5}$ of the plateau modulus with actin concentration[10]. To understand how the elasticity increases on confinement, we have thus to understand how this 'entanglement volume' V_e decreases in response to the confinement constraints.

To this end, we measured the conformations of fluorescently labelled actin filaments, which were polymerized close to the critical polymerization concentration ($c_A = 0.24$ μM). This resulted in emulsion droplets containing only a few actin filaments. When the short-time fluctuations in a plane perpendicular to the (average) polymer axis were followed, the width of the fluctuations A was observed to decrease with decreasing droplet diameter D (Fig. 2a inset). For droplet diameters larger than 30 μm, $A(D)$ levels off, which coincides well with the constant bulk moduli measured for $D > 30$ μm. Assuming a persistence length $l_p \approx 17$ μm, our experimental data for A can be fitted very well with a power law $A = 0.05 D^{3/2} l_p^{-1/2}$ for $D < 30$ μm (Fig. 2a inset), where the constant factor $l_p^{-1/2}$ introduced for dimensional reasons anticipates the theoretical prediction. This relation is different from

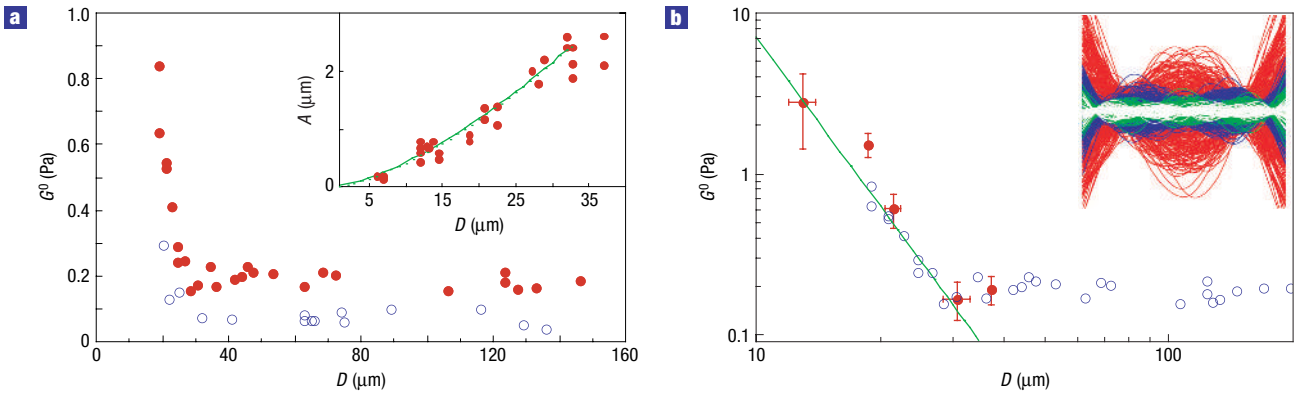

Figure 2 Confinement of actin networks into bio mimetic microcavities of diameters less than the average length of the actin filaments decreases the thermal contour undulations and increases the local network elasticity measured by microscopy and active microrheometry, respectively. a, The effective (locally measured) plateau modulus G^0 as a function of D for actin concentrations of 0.6 mg ml^{-1} (open circles) and 1.2 mg ml^{-1} (filled circles). Inset: The width A of the fluctuations of a confined single filament in a dilute network as a function of the droplet diameter (filled circles) can be fitted with equation (1) with a slightly reduced numerical prefactor as described in the text (line). **b**, Using equation (2), one obtains the plateau shear modulus G^0 either directly from the data for A obtained in the inset of **a** (filled circles) or from the fit to these data (line) in rather good agreement with the microrheological data (open circles, $c_a = 1.2$ mg ml^{-1}, a $r_{A:G} = 7{,}770{:}1$). The data points (filled circles) were obtained by binning (6 μm) the droplet size, the error bars give the standard deviations in the amplitude and droplet size. Inset: snapshots from a Monte Carlo simulation of a weakly bending free single filament with successively more of the longest modes suppressed (from back to front), which illustrates the mechanism underlying the theoretical prediction equation (1) proposed to be responsible for the developing heterogeneities and the accompanying increase of the network elasticity.

the expression $A \propto D^2$ proposed in earlier studies[9], but is consistent with an effective suppression of increasingly higher single-polymer eigenmodes with progressive constriction, which yields (see the Methods section):

$$A \approx 0.1 D^{3/2} l_p^{-1/2} \qquad (1)$$

in agreement with the predicted[18] 'fuzzy diameter' of a semiflexible polymer bent into a ring of diameter D. In view of the experimental difficulty in determining the width of the transverse fluctuations accurately, and given the fact that sometimes more than one single filament was present in the measured drops, the quantitative agreement between the parameter-free equation (1) and the fit in (Fig. 2a inset) is indeed very reasonable.

In more-concentrated solutions, geometrical confinement will act on the polymers in a similar way. However, as the polymers are entangled and therefore strongly interacting, the confining constraints will result in a reorganization of the network structure, which is not *a priori* related to the single-polymer behaviour in a simple way. One expects that with decreasing droplet size, the actin filaments will initially rearrange to minimize their axial confinement, which tends to crowd the centre of the drop. On further reduction of D, the filaments will start to buckle and to coil up on great circles, which will consequently deplete the centre of the drop and tend to crowd its periphery. Altogether, the network should in any case become increasingly heterogeneous on progressive confinement. This expectation is confirmed by the already mentioned increasing width of the measured mesh size distribution with decreasing D. The most spectacular indication for the developing heterogeneities is of course the relatively sudden change in the network structure from central crowding to the crowding of the periphery, that is, the cortex formation below for $D \approx D_c$. For the relatively stiff actin filaments ($L \approx l_p$), it seems plausible that the latter is a consequence of strong filament buckling into semicircular conformations along great circles of the spherical drop, when the diameter D decreases to about $D \approx 2L/\pi \approx 13\,\mu\text{m} \approx 2l_p/\pi$ in good agreement with the observed D_c of 12−13 μm. The corresponding mechanical buckling forces are already substantial for free polymers, namely at least about $\pi^2 k_B T l_p / L^2 \approx 6 k_B T / L$ per filament.

To infer the expected increase in the plateau shear modulus corresponding to these structural rearrangements, we assume that the bulk relation $\xi = d^{5/6} l_p^{1/6}$ between the 'tube diameter' d, which we identify with the fluctuation width A, and the local mesh size ξ remain valid. This results in the following expression for G^0

$$G^0 \propto k_B T l_p^{-2/3} A^{-7/3} \propto k_B T l_p^{1/2} D^{-7/2}. \qquad (2)$$

For the last expression, we have made the further assumption that the concentration dependence of the entanglement effects and the external confinement effects on the fluctuation amplitude A factorize, so that for the dependence of A on D the functional relation established for confined single polymers in equation (1) still holds for higher concentrations. Using the values 1,710 (1.2 mg ml^{-1} actin) and 630 (0.6 mg ml^{-1}) for the suppressed concentration-dependent prefactor in equation (2), respectively, the data for A from Fig. 2a can be matched onto the measured G^0 (Fig. 2b). Thus, equation (2) describes the increase $G^0(D)$ on confinement very well. Moreover, the ratio of the prefactors for the two different actin concentrations is in excellent agreement with the expected power-law increase of $G^0 \sim c_a^{7/5}$, demonstrating the consistency of the factorization assumption. The mechanical effects of confinement on semiflexible polymers in dilute and semidilute solutions thus seem analogous. Interestingly, our measurements of G^0 and ξ as well as our theoretical interpretation all suggest a gradual increase of the network heterogeneity and elasticity with progressive confinement that could hardly have been guessed from microscopy, which is easily misled by the visual impression of an apparently more abrupt structural change in the confined networks at D_c.

In addition to their potential relevance for the fundamental physics of semiflexible polymers, our results indicate that confinement effects in cells might result in viscoelastic behaviour that is quantitatively very different from what is expected from

in vitro bulk measurements. We consistently interpreted our observations in terms of the reduction of the thermal fluctuations of the individual polymers on confinement. As our biomimetic microcavities allow for the controlled addition of actin-binding proteins and other cell constituents, they may become useful for relating the observed macroscopic viscoelastic properties of cells and their functional dependence on the action of various proteins to well-controlled microscopic system parameters[19]. The emulsion-droplet system is also ideal for the encapsulation and characterization of a well-defined small number of polymers, which makes it a promising experimental tool to escort emerging detailed modelling efforts of cortical networks on a molecular level[20–22]. Such a combined approach seems capable of ultimately providing a sound understanding of the physical principles behind the complex behaviour of cytoskeletal polymer networks.

METHODS

G-actin solutions were prepared by dissolving lyophilized G-actin in deionized water and dialysing against fresh G-Buffer (2 mM Tris, 0.2 mM ATP, 0.2 mM $CaCl_2$, 0.2 mM DTT and 0.005% NaN_3) at 4 °C for 24 h. Actin polymerization was initiated by adding one-tenth of the sample volume of a tenfold concentrated F-buffer (20 mM Tris, 20 mM $MgCl_2$, 2 mM $CaCl_2$, 2 mM DTT and 1 M KCl). After gentle mixing, 20 µl of the solution was immediately transferred to 1 ml of a 0.25 mg mol^{-1} SOPG (Avanti Polar Lipids) containing dodecane solution and emulsion droplets (2 vol%) were prepared by vortexing. The negatively charged phospholipids stabilize the droplets against coagulation, inhibit the electrostatic adsorption of actin to the wall and thus mimic the presence of a fluid membrane with essentially no bending undulations. Thus, only well-separated droplets were observed in the microscope. The actin-capping protein gelsolin was isolated from bovine plasma serum (Cooper, 1987 No. 69). The average length of the actin filaments (21 µm) was controlled by adding gelsolin before polymerization[23] and checked in representative drops by fluorescence microscopy. The conformations of the encapsulated filaments were observed by fluorescence microscopy of phalloidin-TRITC (Sigma)-labelled filaments at a very low actin concentration of 0.01 mg ml^{-1}, where single filaments were visible. To prevent oxidation of the fluorophore a standard antioxidant buffer supplement (Glukose–Oxidase, Sigma, 2 mg; Catalase, Fluka, 0.5 mg; and DTT) was used.

The local structure of the actin network in droplets was determined by digital video microscopy and subsequent particle tracking[24] of the thermal motion of incorporated carboxylated latex particles (IDC) with a radius $a = 0.1$ µm comparable to the typical mesh size ξ ($\xi \approx 0.3 c_a^{-1/2}$ µm) of the network[25]. At short times, the latex particles are able to diffuse freely in the local pores, whereas at longer times the diffusion of the particles is slowed down by the presence of the surrounding network. The plateau in the mean-square displacement of individual particles at intermediate times τ can therefore be taken as a measure of the local pore size[26,27] $\xi \approx \sqrt{\langle \Delta x^2(\tau) \rangle} + a$. The resulting pore size distributions were fitted with a gaussian to obtain a mean pore size.

To study the local viscoelastic response of the confined actin network, we used superparamagnetic polystyrene beads (Tosyl activated Dynabeads M-450, Dynal) of a much larger radius $a = 2.25$ µm $\gg \xi$ in a magnetic tweezers setup. Although there has been much debate about the relation of the frequency-dependent 'moduli' measured by microrheometry to those measured by macrorheometry, its has been demonstrated that the plateau shear modulus of actin solutions and gels, which is the quantity that matters most for our quantitative analysis, may be quantitatively determined by the microrheometric technique used[28]. To prevent the apolar polystyrene beads from moving to the dodecane phase, the beads were coated with Protein A (Sigma) according to the procedure provided by the supplier. Actin was polymerized in the presence of the colloidal particles. The emulsion was transferred to a Teflon tube holding a 20 µl measuring chamber. After filling, the measuring chamber was closed by vacuum grease and a spherical plastic coverslip (Polysciences) and put onto the magnetic tweezers setup[29]. Slight adsorption of the droplets to the coverslip prevented droplet movement during the active rheology experiment. The concentration of magnetic particles was adjusted, so that on average only single particles were encapsulated in each emulsion droplet.

We assume that the difference between a confined and a free polymer can be represented very simply by a complete suppression of the thermal fluctuations of the eigenmodes with wavenumber $p_i < p_n = \pi/D$. We denote the corresponding restricted thermal average by $\langle\rangle_n$. Within the Kratky–Porod or worm-like chain model, the corresponding restricted thermal transverse mean square fluctuations $\langle r^2 \rangle_n$ relative to the mean axis of a stiff polymer are then easily calculated:

$$\overline{\langle r^2 \rangle_n} = \sum_{i=n}^{\infty} 2/L l_p p_i^4 \sim 2/3\pi^4 l_p D^3 \Rightarrow A \approx 0.1 D^{3/2} l_p^{-1/2}.$$

We averaged the result along the whole contour (indicated by the overbar), as the amplitude of the fluctuations varies along the polymer as illustrated by the snapshots from Monte Carlo simulations in the inset of Fig. 2b.

Received 22 August 2005; accepted 27 January 2006; published 26 February 2006.

References

1. Kassner, M. E. *et al.* New directions in mechanics. *Mech. Mater.* **37,** 231–259 (2005).
2. Eisenriegler, E. Universal density-force relations for polymers near a repulsive wall. *Phys. Rev. E* **55,** 3116–3123 (1997).
3. Hu, H. W. & Granick, S. Viscoelastic dynamics of confined polymer melts. *Science* **258,** 1339–1342 (1992).
4. Luengo, G., Schmitt, F. J., Hill, R. & Israelachvili, J. Thin film rheology and tribology of confined polymer melts: Contrasts with bulk properties. *Macromolecules* **30,** 2482–2494 (1997).
5. Gardel, M. L. *et al.* Elastic behavior of cross-linked and bundled actin networks. *Science* **304,** 1301–1305 (2004).
6. Shin, J. H., Gardel, M. L., Mahadevan, L., Matsudaira, P. & Weitz, D. A. Relating microstructure to rheology of a bundled and cross-linked F-actin network in vitro. *Proc. Natl Acad. Sci. USA* **101,** 9636–9641 (2004).
7. Helfer, E. *et al.* Microrheology of biopolymer-membrane complexes. *Phys. Rev. Lett.* **85,** 457–460 (2000).
8. Limozin, L. & Sackmann, E. Polymorphism of cross-linked actin networks in giant vesicles. *Phys. Rev. Lett.* **89,** 168103 (2002).
9. Limozin, L., Barmann, M. & Sackmann, E. On the organization of self-assembled actin networks in giant vesicles. *Eur. Phys. J. E* **10,** 319–330 (2003).
10. Hinner, B., Tempel, M., Sackmann, E., Kroy, K. & Frey, E. Entanglement, elasticity, and viscous relaxation of actin solutions. *Phys. Rev. Lett.* **81,** 2614–2617 (1998).
11. Gittes, F. & MacKintosh, F. C. Dynamic shear modulus of a semiflexible polymer network. *Phys. Rev. E* **58,** R1241–R1244 (1998).
12. Morse, D. C. Viscoelasticity of tightly entangled solutions of semiflexible polymers. *Phys. Rev. E* **58,** R1237–R1240 (1998).
13. Kroy, K. Elasticity, dynamics and relaxation in biopolymer networks. *Curr. Opin. Colloid Interface Sci.* published online 20 December 2005 (doi:10.1016/j.cocis.2005.10.001).
14. Mackintosh, F. C., Kas, J. & Janmey, P. A. Elasticity of semiflexible biopolymer networks. *Phys. Rev. Lett.* **75,** 4425–4428 (1995).
15. Gardel, M. L. *et al.* Scaling of F-actin network rheology to probe single filament elasticity and dynamics. *Phys. Rev. Lett.* **93,** 188102 (2004).
16. Isambert, H. *et al.* Flexibility of actin-filaments derived from thermal fluctuations—effect of bound nucleotide, phalloidin, and muscle regulatory proteins. *J. Biol. Chem.* **270,** 11437–11444 (1995).
17. Morse, D. C. Viscoelasticity of concentrated isotropic solutions of semiflexible polymers. 2. Linear response. *Macromolecules* **31,** 7044–7067 (1998).
18. Odijk, T. DNA in a liquid-crystalline environment: Tight bends, rings, supercoils. *J. Chem. Phys.* **105,** 1270–1286 (1996).
19. Noireaux, V. & Libchaber, A. A vesicle bioreactor as a step toward an artificial cell assembly. *Proc. Natl Acad. Sci. USA* **101,** 17669–17674 (2004).
20. Wilhelm, J. & Frey, E. Elasticity of stiff polymer networks. *Phys. Rev. Lett.* **91,** 108103 (2003).
21. Head, D. A., Levine, A. J. & MacKintosh, F. C. Distinct regimes of elastic response and deformation modes of cross-linked cytoskeletal and semiflexible polymer networks. *Phys. Rev. E* **68,** 061907 (2003).
22. Heussinger, C. & Frey, E. Stiff polymers, foams and fiber networks. *Phys. Rev. Lett.* **96,** 017802 (2006).
23. Janmey, P. A. *et al.* The mechanical-properties of actin gels — elastic-modulus and filament motions. *J. Biol. Chem.* **269,** 32503–32513 (1994).
24. Schilling, J., Sackmann, E. & Bausch, A. R. Digital imaging processing for biophysical applications. *Rev. Sci. Instrum.* **75,** 2822–2827 (2004).
25. Schmidt, C. F., Barmann, M., Isenberg, G. & Sackmann, E. Chain dynamics, mesh size, and diffusive transport in networks of polymerized actin—a quasielastic light-scattering and microfluorescence study. *Macromolecules* **22,** 3638–3649 (1989).
26. Valentine, M. T. *et al.* Investigating the microenvironments of inhomogeneous soft materials with multiple particle tracking. *Phys. Rev. E* **64,** 061506 (2001).
27. Wong, I. Y. *et al.* Anomalous diffusion probes microstructure dynamics of entangled F-actin networks. *Phys. Rev. Lett.* **92,** 178101 (2004).
28. Gardel, M. L., Valentine, M. T., Crocker, J. C., Bausch, A. R. & Weitz, D. A. Microrheology of entangled F-actin solutions. *Phys. Rev. Lett.* **91,** 158302 (2003).
29. Keller, M., Schilling, J. & Sackmann, E. Oscillatory magnetic bead rheometer for complex fluid microrheometry. *Rev. Sci. Instrum.* **72,** 3626–3634 (2001).

Acknowledgements

We thank M. Rusp for the actin preparation. We are grateful for the discussions with E. Frey, C. Heussinger and M. Bathe. The work was supported by SFB563 and SFB 413 and partly by the 'Fonds der Chemischen Industrie'.
Correspondence and requests for materials should be addressed to A.R.B.
Supplementary Information accompanies this paper on www.nature.com/naturephysics.

Competing financial interests

The authors declare that they have no competing financial interests.